Phys. Status Solidi C **13**, No. 10–12, 712–717 (2016) / **DOI** 10.1002/pssc.201600016

physica status solidi c
www.pss-c.com
current topics in solid state physics

The nature of boron-oxygen lifetime-degrading centres in silicon

Vladimir Voronkov* **and Robert Falster****

SunEdison Semiconductor, via Nazionale 59, 39012 Merano, Italy

Received 13 April 2016, revised 9 May 2016, accepted 10 May 2016
Published online 18 May 2016

Keywords silicon, boron, oxygen, light-induced degradation

* Corresponding author: e-mail vvoronkov@sunedisonsemi.it, Phone: +39 0473 333 308, Fax: +39 0473 333 270
** e-mail rfalster@sunedisonsemi.it, Phone: +44 1993 810 784

Light-induced degradation of minority carrier lifetime in silicon is caused by the formation of two B-O recombination centres: fast-stage centres (FRC) and slow-stage centres (SRC). FRC were concluded to emerge by a carrier-assisted reconfiguration of a latent BO_2 defect composed of a substitutional boron atom and an oxygen dimer. The nature of SRC however remained uncertain; this defect appeared to involve an interstitial boron atom rather than a substitutional one. More recent data on SRC in boron-containing compensated p-Si and n-Si now show that the SRC actually emerge in the same way as FRC: by a re-configuration of BO_2, but from a different latent form. The two latent BO_2 defects (the precursors for FRC and for SRC) are created during a cooling stage after the last high-temperature anneal, and their concentration, proportional to the boron concentration and squared oxygen concentration, depends on the cooling rate.

1 Introduction Minority carrier lifetime in boron and oxygen containing silicon degrades severely in the presence of excess carriers – in both p-Si [1-6] and n-Si [7-11]. This phenomenon is of crucial importance for the efficiency of solar cells. The boron-oxygen recombination centres emerge in two stages [5], and have been accordingly labelled FRC (fast stage recombination centre) and SRC (slow stage recombination centre). In non-compensated p-Si, the saturated concentration of both centres was found [5] to be proportional to the boron concentration N_B and to the squared oxygen concentration C_{ox}^2. After a prolonged illumination, the dominant contribution into the recombination rate is due to SRC. Initially the B-O recombination centres were assumed [3-5] to be BO_2 defects that appear, in the course of illumination, due to trapping of oxygen dimers O_2 by substitutional boron atoms B. However, the degradation rate constant in compensated p-Si [6] was found to depend on the hole concentration p_0 and not on the boron concentration N_B. This shows that the centres are actually produced by a hole-assisted reconfiguration of some latent (recombination-inactive) B-O defects into recombination-active form [12]. The latent state for FRC production is denoted FLC and that for SRC production – SLC.

In boron-containing n-Si, the saturated FRC concentration [9] is close to the concentration found in p-Si for the same N_B and C_{ox}. It was thus concluded that the FRC is a BO_2 defect, composed of a substitutional boron atom B and an oxygen dimer. The difference from the initial model [3-5] is that the BO_2 defect, in its latent form, is already present prior to degradation having been created during the cooling stage following the prior high-temperature anneal. Such an anneal may be any number of things: a thermal donor killing or a phosphorus diffusion/gettering treatment for example. During illumination (more generally, in the presence of excess carriers) the latent BO_2 (FLC) defect is activated, by a carrier-assisted re-configuration into FRC.

The nature of SLC (the precursor for SRC) seemed, for a long time, to be much more complicated. Several research groups [6, 13-15] reported that the saturated SRC concentration in compensated p-Si correlates not to N_B but rather to the hole concentration p_0 (the net doping). This feature could be explained [12] assuming that the B-O precursor of SRC involves an interstitial boron atom B_i rather than the substitutional one. The B_i atoms, produced by self-interstitials emitted by growing oxygen precipitates, were assumed to be mostly clustered into nano-precipitates; the dissolved B_i component is then proportional to p_0, due to the single-positive charge of B_i in p-Si. In non-compensated p-Si co-doped with B and Ga, the SRC concentration was found to definitely correlate to N_B and not

to p_0 [16] but this could be explained by competing trapping of B_i by B and Ga [17].

In the present work, we consider more recent data on SRC and conclude that the latent precursors for both recombination centres, SRC and FRC, are similar: they are two different configurations of the BO_2 defect.

2 Concentration of B-O in p-Si and n-Si

2.1 SRC in compensated p-Si Contrary to the previous works [6, 13-15], a subsequent study of lifetime degradation in compensated p-Si [18] revealed that the saturated SRC concentration follows the same dependence on N_B that has been earlier found in non-compensated p-Si [5]. The discrepancy with previous works (that claimed a correlation to p_0) was reasonably attributed [18] to a poorly controlled value of C_{ox} in those works.

2.2 SRC in compensated n-Si In boron-containing compensated n-Si, the hole-assisted production rate of FRC and SRC is strongly retarded since holes are now the minority carriers of a concentration far lower than in p-Si material. In the first experiments, using a relatively small light intensity [9] (and hence a small excess hole concentration), only the FRC production stage (a faster process) could be traced. FRC was concluded to be a two-level defect, with a donor level in the upper half of the gap and an acceptor level in the lower half of the gap (which corresponds to a negative-U centre). In a more recent study of such a material [10, 11], using a higher light intensity, the SRC production stage could be traced. SRC was concluded to be, similar to FRC, a two-level negative-U centre, and the saturated effective concentration of SRC was found to be insensitive to a widely varied net doping n_0.

2.3 Comparison of SRC saturated concentration in n-Si and p-Si The concentration M of either recombination defect, FRC or SRC, can only be deduced from lifetime data in combination with one of the four capture coefficients, two for the donor level (α_{nd} of electron capture by the positive charge state, and α_{pd} of a hole capture by the neutral state) and two for the acceptor level (α_{na} of an electron capture by the neutral state, and α_{pa} of a hole capture by the negative state). Different definitions have been used previously [9-11]. In the present paper, the effective concentration is defined as $\alpha_{nd}M$ and denoted N_{nd}. If the reported effective concentrations correspond to a different definition they can be recalculated by multiplying them by a proper ratio of the capture coefficients. For instance the SRC effective concentration N_{pd}, defined through α_{pd} [11], should be multiplied by $Q_d = \alpha_{nd}/\alpha_{pd}$. The capture ratio Q_d for the donor level of SRC was reported to be about 10 [2, 5].

In p-Si, the expression for the SRC-controlled lifetime τ_{src}, in dependence of the injection ratio $x = n/p$ (where n and p are the actual concentrations of electrons and holes, and $p = p_0 + n$) reads [9, 19]:

$$1/\tau_{src}=N_{nd}\,(1+xQ_{ad})/[1+xQ_d\,(1+p_a/p_0-n_d/p_0)-x^2Q_d\,p_a/p_0], \quad (1)$$

where $Q_{ad} = \alpha_{na}/\alpha_{pd}$ is the capture ratio for the neutral charge state deduced to be 0.55 [10], n_d is the electron concentration for the Fermi level at the donor level E_d and p_a is the hole concentration for the Fermi level at the acceptor level E_a. By Eq. (1), the effective concentration N_{nd} has a simple meaning: it is equal to the SRC-controlled reciprocal lifetime in p-Si, in the limit of a low injection level ($x << 1/Q_d$).

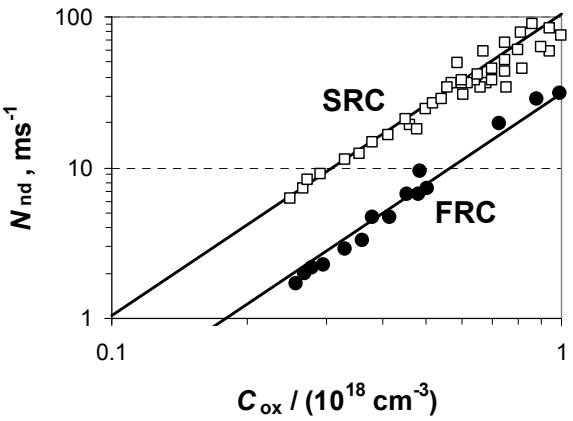

Figure 1 Effective concentration N_{nd} (reduced to a standard boron content $N_d = 10^{16}$ cm^{-3}) for SRC and FRC in non-compensated p-S in dependence on the oxygen concentration C_{ox} based on the data of Ref. [5]. The solid lines correspond to a square dependence on C_{ox}.

The SRC energy levels have been reported to be quite deep: $E_d = 0.41$ eV [2] (referenced from the bottom of the conduction band) and $E_a = 0.26$ eV [10] (referenced from the top of the valence band). If the lifetime is measured near T_{room}, both n_d ($\approx 3.5\times10^{12}$ cm^{-3}) and p_a ($\approx 4\times10^{14}$ cm^{-3}) are small in comparison to a representative value of p_0 (about 10^{16} cm^{-3}), and Eq. (1) is simplified:

$$1/\tau_{src} = N_{nd}\,(1 + Q_{ad}\,x) / (1 + Q_d\,x). \quad (2)$$

The reported values of τ_{src} in p-Si for a specified injection ratio x (usually, about 0.1) can be converted into N_{nd} using Eq. (2). In n-Si, a more complicated expression for the lifetime, through an injection ratio $y = p/n$, should be used to deduce N_{nd} [9, 10, 19].

Fig. 1 shows the effective concentration N_{nd} of SRC and FRC deduced from the lifetime data of Ref. [5] for non-compensated p-Si.

In Fig. 2, the values of N_{nd} for SRC in non-compensated p-Si and compensated n-Si are presented in dependence of N_B, for a reference oxygen concentration $C_{ox} = 7\times10^{17}$ cm^{-3} (if the actual C_{ox} is different, N_{nd} was corrected using a square dependence on C_{ox}). The solid line represents re-

sults by Bothe and Schmidt for non-compensated p-Si [5] which have been just shown in Fig. 1. The broken line represents the corrected (reduced) values [4] for the case of phospurus-diffused samples. The open symbols correspond to more recent degradation data on non-compensated p-Si

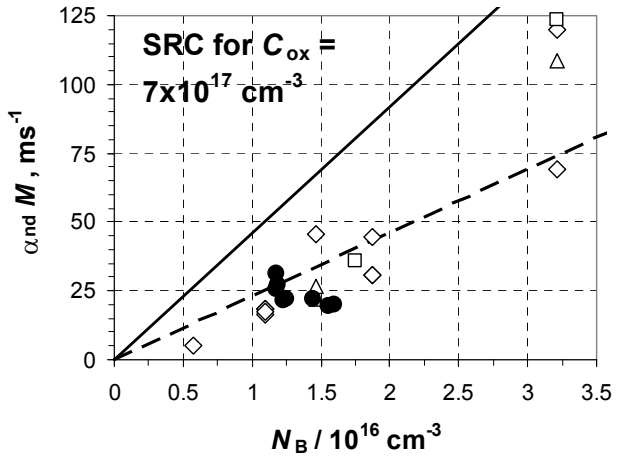

Figure 2 The effective saturated concentration N_{nd} for SRC in dependence of the boron concentration N_B. Lines and open symbols are for non-compensated p-Si, filled circles are for compenstated n-Si.

(the raw data have been provided by courtesy of Lim). The filled circles are the values of N_{nd} for n-Si samples based on the data of Ref. [11]. Although the scatter is significant (roughly, by a factor of 2 or even more), all the data overlap and fall into the same proportional dependence of N_{nd} on N_B.

2.4 Comparison of FRC in n-Si and p-Si For the sake of completness, a plot similar to Fig. 2 is shown also for FRC (Fig. 3); the data again refer to a standard value of $C_{ox} = 7\times10^{17}$ cm^{-3}. The filled symbols correspond to the saturated FRC concentration found in n-Si: the circles are based on the data of Ref. [11], and the single filled square (in the upper-right part) is the recalculated value from Ref. [9]. The solid and broken lines (similar to those in Fig. 1) represent the FRC concentration in non-compensated p-Si [5]. The reported τ_{frc} is related to the effective concentration $N_{nd} = \alpha_{nd}M$ by the same Eq. (2) – now applied to FRC, but of course with different values of the parameters: $Q_d = 65$ and $Q_{ad} = 0.13$ [9]. The FRC concentration for phosphorus-diffused samples (the broken line in Fig. 3) is shown assuming the same reduction factor as for SRC. In spite of a considerable scatter, the FRC concentration is clearly similar for n-Si and p-Si at comparable N_B. This feature lead [9] to the identification of FRC as a form of a BO_2 defect.

2.5 The nature of SRC We conclude that on average (within a scatter) the saturated concentration of both SRC and FRC follows a simple dependence on the material parameters: they are both just proportional to N_B and to C_{ox}^2. The nature of SRC and FRC centres is then similar: each centre originates from its own latent configuration of BO_2. An oxygen dimer can exist in several atomic configurations [20], and we can expect even a more rich configurational variety for a BO_2.

Light-induced lifetime degradation can now be described in the following simple way. Initially (before degradation) there are two different latent configurations of BO_2 defects inherited from the preceding anneals. These two latent states correspond to FLC and SLC. In the presence of excess carriers, FLC reconfigures into recombination-active state FRC, and SLC independently reconfigures into another recombination-active state, SRC.

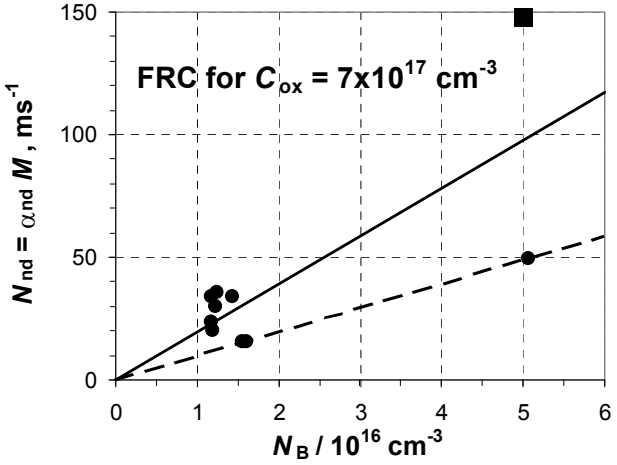

Figure 3 The effective saturated concentration N_{nd} for FRC in dependence of the boron concentration N_B. Lines are for non-compensated p-Si, filled symboles (circles and a square) are for compenstated n-Si.

The degree of degradation is controlled by the concentrations of the latent BO_2 defects, in two structural forms FLC and SLC (mostly, SLC for fully degraded samples). Each concentration, M_f (of BO_2-FLC) and M_s (of BO_2-SLC) is inherited from the thermal history. In particular, if a high-T anneal is applied prior to degradation, the latent BO_2 defects are created during a cooling stage after this anneal. Each frozen-in concentration is proportional to $N_B C_{ox}^2$ for a fixed cooling temperature profile. Now we consider an important issue of the cooling rate effect on the frozen-in BO_2 concentration.

3 Frozen-in BO_2 concentration

3.1 Kinetic equations for BO_2 production The evolution of the BO_2 concentration M (omitting a subscript f or s, since the equations are the same for both kinds of BO_2) is described by a diffusion-limited pairing/dissociation reaction of O_2 and B:

$$dM/dt = 4\,\pi\, r\, D_2\, (C_2\, N_B - K\, M), \quad (3)$$

where D_2 and C_2 are the diffusivity and concentration of O_2, and K is the equilibrium dissociation constant for the pairing reaction that can be expressed through the binding energy E of the two interacting defects B and O_2:

$$K = (\rho/Z)\, \exp(-E/kT). \quad (4)$$

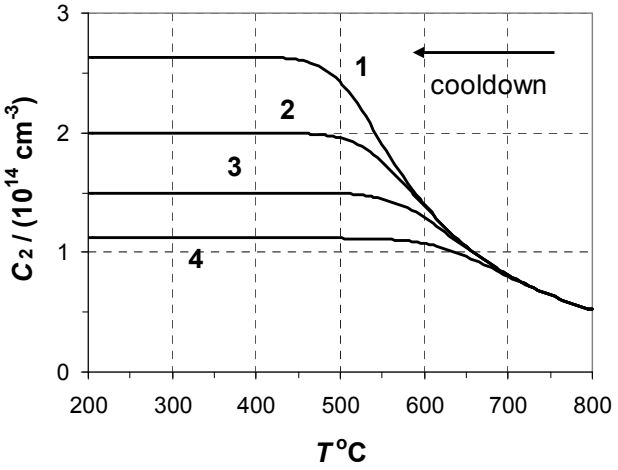

Figure 4 Calculated concentration of oxygen dimers during a cooldown. Curves 1 to 4 are for different cooling rates: 0.1, 1, 10 and 100 K/s, respectively.

Here, ρ is the lattice site density (5×10^{22} cm^{-3}) and Z is the number of equivalent configurations of O_2 around B. We tentatively take $Z = 4$ although it can be larger, depending on the structure of O_2. The binding energy E is specific for each BO_2 form.

The concentration of O_2 changes by a kinetic equation similar to Eq. (3):

$$dC_2/dt = 4\,\pi\, r\, D_{ox}\, (C_{ox}^2 - K_2\, C_2), \quad (5)$$

where D_{ox} is the monomeric oxygen diffusivity [21] and K_2 is the equilibrium dissociation constant of O_2. The values of $K_2(T)$ and $D_2(T)$ have been deduced using the data on dislocation locking by oxygen dimers [22] and the transient generation kinetics of thermal donors [23] limited by the accumulation of O_2 (which are the precursors for the thermal donors).

The computed evolution of C_2 is shown in Fig. 4 for several cooling rates. Initially C_2 increases closely following the equilibrium value $C_{2e} = C_{ox}^2/K_2$. Later (below 500 to 600 °C, depending on the cooling rate) the pairing rate of oxygen into O_2 becomes too slow to further increment C_2, and a definite value of the dimeric concentration (proportional to C_{ox}^2) is frozen-in.

3.2 Evolution of BO_2 in a course of cooling The equation system (3) and (5) can be numerically solved for any specified cooling rate $q = -dT/dt$ and different assumed values of the binding energy E. An example of computed evolution of the BO_2 concentration M (normalized by the boron concentration N_B), in the course of cooling, is shown in Fig. 5 for several values of E. This plot demonstrates a high sensitivity of the frozen-in concentration M to the value of the BO_2 binding energy E. The computed curves are for a representative oxygen concentration $C_{ox} = 7\times10^{17}$ cm^{-3} and for the cooling rate q fixed at 1 K/s (a tentative value for cooling after phosphorus gettering step). For the capture radius r in both Eqs. (3) and (5), a conventional value 0.3 nm was used.

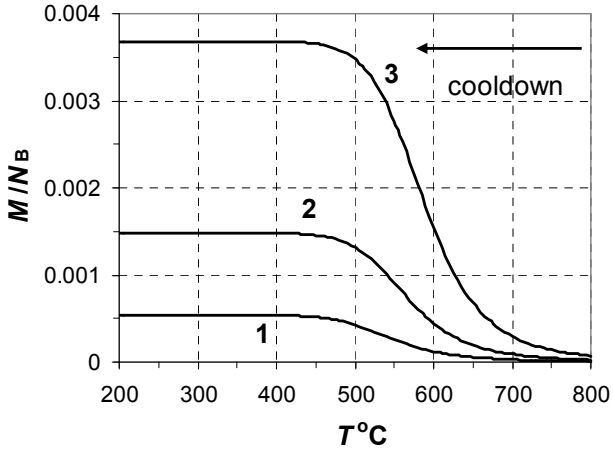

Figure 5 Computed evolution of normalized BO_2 concentration upon cooldown from 800 °C with a cooling rate 1 K/s. The curves 1 to 3 are for three different values of assumed BO_2 binding energy: $E = 0.7$, 0.8 and 0.9 eV, respectively.

Initially the BO_2 concentration increases remaining close to the equilibrium value $M_e = C_2\, N_B/K$. Later, due to a reduced D_2, the pairing rate becomes too low to further increment M, and the BO_2 concentration is then frozen-in, as manifested in Fig. 5 by a low-T plateau in $M(T)$.

3.3 Effect of cooling rate on frozen-in BO_2 The computed frozen-in normalized concentration M/N_B in dependence of the cooling rate is shown in Fig. 6, for the same three values of E as in Fig. 5. The cooling rate was assumed to be the same over the whole range of T. Actually, only the relevant temperature range where freezing-in occurs is important; this is a range from 550 down to 450 °C. An increase in the cooling rate, in this range, by a factor of 10 leads to a reduction in the frozen-in concentration M by a factor of ≈ 2.5. This corresponds to a power-type dependence, $M \sim 1/q^{0.4}$. At a high cooling rate such as 100 K/s (which may be achieved by firing in a belt furnace [24]) the frozen-in BO_2 concentration is reduced significantly.

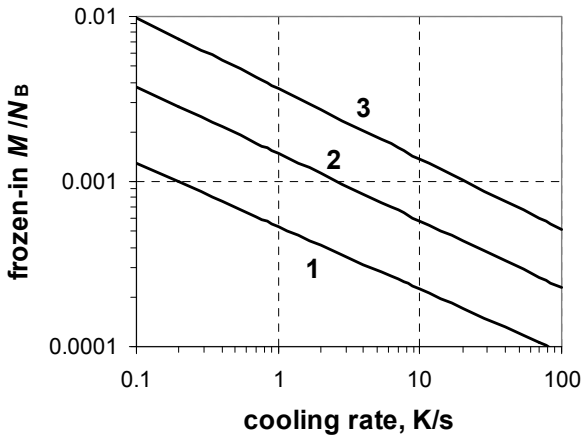

Figure 6 Dependence of the frozen-in normalized BO_2 concentration on the cooling rate. The three curves 1 to 3 correspond to the same values of the BO_2 binding energy as those in Fig. 5: E = 0.7, 0.8 and 0.9 eV, respectively.

Samples subjected to degradation tests have usually been pre-annealed at some high T (well above 500 °C). The sample cooling rate (at around 500 °C) following this anneal is an important parameter and one that should be traced or at least fixed, for a better control of the subsequent degradation amplitude. In most previously reported works, the cooling curve was, unfortunately, not well specified. This could be one of the reasons for a large scatter in the deduced FRC and SRC concentrations.

4 Absolute concentration of BO_2

4.1 Capacitance data on FRC From lifetime data, only a product of the centre concentration M and a capture coefficient (like α_{nd}) can be deduced while the individual values of M and α_{nd} cannot be found separately. However, if M is reasonably high, it can be determined by electrical measurements.

The latent BO_2 defects are likely to be acceptors (negative defects) similar to B. During degradation, they reconstruct into FRC and SRC which have a donor level in the upper half of the gap and thus exist as positively charged defects in p-Si, in the dark. Hence, degradation leads to a decrease in the net acceptor concentration N_a, from $N_B + M$ before degradation down to N_B–M after. Indeed, a measurable reduction in N_a, by about 0.4%, was found by a capacitance technique [25] after a short illumination. By subsequent dark annealing, N_a returns to its initial value within 100 s at 137 °C. It is known that the FRC and SRC are deactivated by dark annealing [5, 26], due to backward reconfiguration into latent state. The reported dark recovery of N_a is far faster than the known dark deactivation rate of SRC [26], and the disappearance of light-induced donors can be thus attributed to a dark recovery of FRC. The estimated M/N_B ratio is 0.002, by the relative capacitance change. The corresponding concentration of BO_2 (here, the precursors for FRC) is ~ 2×10^{13} cm^{-3}, for a standard boron concentration of 10^{16} cm^{-3}. With a roughly known effective concentration $\alpha_{nd}M$ ~ 20 ms^{-1} (Fig. 1 and 3) we can now estimate the capture coefficient of electrons by positive state of FRC: α_{nd} ~ 10^{-9} cm^3/s (the capture cross section is then ~ 10^{-16} cm^2).

The estimated value of $M/N_B \approx 0.002$ allows us to define the binding energy of the BO_2-FLC defect, using the curves shown in Fig. 5 and similar curves computed for other values of E. The frozen-in M/N_B ratio is equal to 0.002 at $E \approx 0.83$ eV. For BO_2-SLC the value of E is unknown but it is likely to be similar - implying a similar concentration M and a similar capture coefficient (cross-section).

4.2 DLTS data In the degraded state, the concentration of FRC (and probably of SRC too) is relatively high, on the order of 2×10^{13} cm^{-3}. And yet attempts to detect light-induced recombination centres by DLTS have been unsuccessful [27]. Recent preliminary findings [28] suggest that a reason could be a passivation of these defects by hydrogen during preparation of test diodes. A more fundamental reason is that both FRC and SRC are two-level negative-U defects. The emission energy of electrons by a negative charge state is $E_g - E_a$ where E_g = 1.2 eV is the gap width; this emission energy is ≈ 0.9 eV for both FRC and SRC. The emission energy of holes by a positive charge state is $E_g - E_d$, roughly 0.8 eV for both FRC and SRC. With such large emission energies, the carrier emission rate around T_{room} is negligible for fully recharged defects (into positive or negative states), giving no DLTS signal. Only neutral states give rise to emission, of both electrons and holes.

5 Summary The B-O recombination centres (FRC and SRC), responsible for the light-induced degradation of the carrier lifetime in Si and thus for the solar cell efficiency loss, presented a long-standing puzzle regarding their origin and chemical composition. An initial model [3-5] attributed these centres to a carrier-enhanced diffusion of oxygen dimers O_2 which leads to their trapping by boron atoms B, in the course of illumination. The FRC and SRC were thus thought to be BO_2 defects composed of a substitutional boron atom and an oxygen dimer. But the data on degradation rate constant in compensated p-Si turned out to be inconsistent with this mechanism [6, 12].

Recent data on the saturated concentrations of FRC and SRC - discussed in the present work - however show that both centres are likely to be indeed BO_2 defects, in two different recombination-active configurations. Yet the origin of these defects is quite different from the initial notion: the BO_2 defects are already present, prior to a degradation run, in two latent (recombination-inactive) forms denoted FLC and SLC. Lifetime degradation is essentially an activation of these latent defects, by their carrier-assisted reconfiguration into recombination-active states, FRC and SRC. The latent BO_2 defects (the precursors for

FRC and SRC) are created in the course of anneals preceding a degradation run, such as a thermal donor killing (at around 650 °C) or phosphorus diffusion/gettering (at around 850 °C), or a firing anneal in a belt furnace (with a peak temperature at around 800 °C). At high T, the BO_2 concentration, M, corresponds to equilibrium with respect to B + O_2 pairing/dissociation; it is proportional to the boron concentration N_B and to the squared oxygen concentration C_{ox}^2. At a later stage of cooling, at lower T, the equilibrium is no longer supported, due to reduced diffusivity of oxygen dimers and monomers. Hence a definite value of M (proportional to $N_B C_{ox}^2$) is frozen-in by a cooldown. This frozen-in value of M depends on the cooling rate in a relevant temperature interval of freezing, which is roughly 550 °C down to 450 °C. The dependence of frozen-in M on the cooling rate $q = -dT/dt$ is not very strong and yet well pronounced, following a power dependence $M \sim 1/q^{0.4}$.

Lifetime data give only the effective concentration of BO_2, a product of the true concentration M and one of the carrier capture coefficients. The absolute value of M for FRC can be independently estimated by a reported [25] light-induced capacitance change: the M/N_B ratio is roughly 0.002. The absolute value of the capture coefficient α_{nd} (of electrons by the positive charge state of FRC) can thus be estimated; the corresponding capture cross-section is about 10^{-16} cm^2. For SRC, the absolute values of the concentration and the capture coefficients are not yet known but they are likely to be similar to those of FRC.

The identification of FLC/FRC and SLC/SRC defects as different configurations of BO_2 is the simplest possible model consistent with the data on the saturated concentrations of FRC and SRC. The defect composition could be yet more complicated, involving for instance a fast-diffusing impurity (like Cu) denoted X [17]. The recombination defects would be then XBO_2, with a BO_2 defect as a core. The reaction sequence, in the course of sample cooling, would be first formation of BO_2 and then (at a lower T) attachment of the mobile component X. If the X species is mostly precipitated (into nano-precipitates, NPs), the dissolved concentration of X is a function of only T in the range of intrinsic conductivity. The frozen-in concentration of XBO_2 would be proportional to that of BO_2 showing the same dependence on B and O concentrations.

Acknowledgements We are grateful to Bianca Lim and Dominic Walter of ISFH (Hamelin) and Tim Niewelt of the Fraunhofer ISE Institute (Freiburg) for discussions of their data on lifetime degradation.

References

[1] H. Fischer and W. Pshunder, Proc. 10th IEEE Photovoltaic Conference, p. 404 (1974).
[2] S. Rein and S.W. Glunz, Appl. Phys. Lett. **82**, 1054 (2003).
[3] J. Schmidt and K. Bothe, Phys. Rev. B **69**, 024107 (2004).
[4] K. Bothe, R. Sinton, and J. Schmidt, Prog. Photovolt.: Res. Appl. **13**, 287 (2005).
[5] K. Bothe and J. Schmidt, J. Appl. Phys. **99**, 013701 (2006).
[6] D. Macdonald, F. Rougieux, A. Cuevas, B. Lim, J. Schmidt, M. Di Sabatino, and L.J. Geerling, J. Appl. Phys. **105**, 093704 (2009).
[7] B. Lim, F. Rougiex, D. Macdonald, K. Bothe, and J. Schmidt, J. Appl. Phys. **108**, 103722 (2010).
[8] T. Schutz-Kuchly, S.B. Dubois, J. Veirman, Y. Veschetti, D. Heslinga, and O. Palais, Phys. Status Solidi A **208,** 572 (2010).
[9] V.V. Voronkov, R. Falster, K. Bothe, B. Lim, and J. Schmidt, J. Appl. Phys. **110**, 063515 (2011).
[10] T. Niewelt, J. Schon, J. Broisch, W. Warta, and M.C. Schubert, Phys. Status Solidi RRL **9**, 692 (2015).
[11] J.Schon, T.Niewelt, J.Broisch, W.Warta and M.C.Schubert, J. Appl. Phys. **118**, 245702 (2015).
[12] V.V. Voronkov and R. Falster, J. Appl. Phys. **107**, 053509 (2010).
[13] R. Kopecek, J. Arumughan, K. Peter, E.A. Good, J. Libat; M. Acciarri, and S. Binetti, Proc. 23rd European Photovolatic Solar Energy Conference, p. 1855 (2008).
[14] B. Lim, F. Rougieux, D. Macdonald, K. Bothe, and J. Schmidt, J. Appl. Phys. **108**, 103772 (2010).
[15] J. Gelker, W. Kwapil, and S. Rein, J. Appl. Phys. **109**, 053718 (2011).
[16] M. Forster, E. Fourmond, F.E. Rougiex, A. Cuevas, R. Gotoh, K. Fujiwara, S. Uda, and M. Lemiti, Appl. Phys. Lett. **100**, 042110 (2012).
[17] V.V. Voronkov and R. Falster, Solid State Phenom. **205-206**, 3 (2014).
[18] M. Forster, P. Wagner, J. Degoulange, R. Einhaus, G. Galbiati, F.E. Rouggiex, A. Cuevas, and E. Fourmond, Sol. Energy Mater. Sol. Cells **120**, 390 (2014).
[19] J.D. Murphy, K. Bothe, R. Krain, V.V. Voronkov, and R.J. Falster, J. Appl. Phys. **111**, 113709 (2012).
[20] J. Coutinho, R. Jones, P.R. Briddon, and S. Oberg, Phys. Rev. B **62**, 10824 (2000).
[21] J.C. Mikkelsen, Mater. Res. Symp. Proc. **59**, 19 (1986).
[22] S. Senkader, P. Wilshaw, and R. Falster, J. Appl. Phys. **89**, 4803 (2001).
[23] V.V. Voronkov, G.I. Voronkova, A.V. Batunina, V.N. Golovina, R. Falster, M. Cornara, N.B. Tiurina, and A.S. Guliaeva, Solid State Phenom. **156-158**, 115 (2010).
[24] D. Walter, B. Lim, K. Bothe, R. Falster, V.V. Voronkov, and J. Schmidt, Sol. Energy Mater. Sol. Cells **131**, 51 (2014).
[25] R.S. Crandall, J. Appl. Phys. **108**, 103713 (2010).
[26] B. Lim, V.V. Voronkov, R. Falster, K. Bothe, and J. Schmidt, Appl. Phys. Lett. **98**, 162104 (2011).
[27] V.P. Markevich, A.R. Peaker, B. Hamilton, L. Murin, Y.H. Yoon, and G. Rozgonyi, Proc. 22th Workshop on Crystalline Silicon Solar cells and Modules, p. 103 (2012).
[28] T. Mchedlidze and J. Weber, Phys. Status Solidi RRL **9**, 108 (2015).